The law of surrounding rock deformation and surface settlement of shield tunnel passing through upper soft and lower hard rock

Guangming Yu
Qingdao University of Technology, School of Civil Engineering
Yongyi Zhang
Qingdao University of Technology, School of Civil Engineering
Yinqiu Bai (550885461@qq.com)
Qingdao University of Technology, School of Civil Engineering
Jun Lei
China Construction Fifth Engineering Bureau
Zihan Yang
China Construction Fifth Engineering Bureau
Gang Li
Qingdao University of Technology, School of Civil Engineering
Bin Peng
China Construction Fifth Engineering Bureau
Lijun Kuang
China Construction Fifth Engineering Bureau
Guanwen Liang
Zhejiang University College of civil engineering and architecture
Weiting Luo
China Construction Fifth Engineering Bureau
Ze Chen
China Construction Fifth Engineering Bureau

Research Article

Keywords: Upper soft and lower hard formation, soft and hard rock junction surface inclination, shield tunnel, surrounding rock plastic yield, surrounding rock deformation

Posted Date: September 27th, 2022

DOI: https://doi.org/10.21203/rs.3.rs-2099219/v1

Additional Declarations: No competing interests reported.

The law of surrounding rock deformation and surface settlement of shield tunnel passing through upper soft and lower hard rock

Guangming Yu[1]，Yongyi Zhang[2]，Yinqiu Bai[1]，Jun Lei[3]，Zihan Yang[3]，Gang Li[1]，Bin Peng[3]，Lijun Kuang[3]，Guanwen Liang[4]，Weiting Luo[3]，Ze Chen[3]

[1]Qingdao University of Technology, School of Civil Engineering，Qingdao,266400，[2]Weichai Power，[3]China Construction Fifth Engineering Bureau,Changsha 410007，[4]Zhejiang University，College of civil engineering and architecture

Abstract: With the rapid increase in the number of urban subway construction in China, the geological distribution encountered in the tunnel construction process is gradually diversified, especially when the excavation is carried out in the upper soft and lower hard formations, there are certain differences in the physical and mechanical properties of the tunnel palm surface, the surrounding rock and the distribution position of the soft and hard rock junction surface, which can easily lead to the occurrence of large deformation or even collapse of the surrounding rock of the tunnel. In order to study the deformation of surrounding rock and the change of surface settlement when the shield tunnel crosses the upper soft and lower hard strata, relying on the actual project of the shield tunnel crossing the upper soft and lower hard strata of Shenzhen metro line 13. Firstly, based on the molar stress circle theory and the theory of elastic mechanics, the influence of internal friction angle and cohesion on the surrounding rock stress is analyzed, and the first yield location and distribution characteristics of the surrounding rock stress of the upper soft and lower hard strata are divided based on the calculation formula of the surrounding rock stress; Secondly, the inclination angle of the soft and hard rock junction surface of the above soft and hard formations is α variable, and the MIDAS GTS NX numerical simulation software is used to set seven working conditions of 0°, 15°, 30°, 45°, 60°, 75°, 90°, and analyze the influence of inclination on the surrounding rock stress of the tunnel, the plastic yield position of the surrounding rock, and the deformation of the surrounding rock. Finally, the surrounding rock deformation and surface settlement monitoring data after the completion of the construction of the soft and lower hard strata in the Liu~Bai section of Shenzhen Metro Line 13 are summarized, and the numerical simulation is compared and analyzed to verify the accuracy of the numerical simulation results, and the final research results can provide a certain reference for similar projects in the later stage.

Key words: Upper soft and lower hard formation; soft and hard rock junction surface inclination; shield tunnel; surrounding rock plastic yield; surrounding rock deformation

Fundings: The research of G.Y. was funded by the National Natural Science Foundation of China (no. 52171264) and NSFC-RFBR (no. 5191101589). The research of J.L. was funded by the Funded by China State Construction Engineering Corporation Technology R&D Program (no.CSCEC-2020-Z-49).

1 INTRODUCTION

According to the basic concept of upper soft and lower hard stratum [1], when the tunnel is constructed in the upper soft and lower hard stratum, the excavation surface and the rock and soil mass of

the excavation extension stratum have certain heterogeneity, and their physical and mechanical properties are quite different. In this case, the tunnel surrounding rock is very easy to produce instability, and even tunnel collapse in serious cases. Therefore, the study on the failure mechanism and characteristics of tunnel surrounding rock in upper soft and lower hard strata has become one of the focuses and hot spots of scholars at home and abroad. 10. X. Y. Lei, Swoboda[2] and others analyzed the soft-hard rock interface in tunnel excavation by using the finite element simulation software. The results show that the shear force and deformation of the supporting structure near the interface are increasing. Yassaghi[3] used the UDEC software to analyze the distribution of the plastic zone of the tunnel surrounding rock and the tunnel face in the soft-hard composite stratum. Wang Wei[4] and others analyzed the stability of surrounding rock of tunnel in upper soft and lower hard stratum by means of numerical simulation. The results show that: under the influence of tunnel excavation and unloading, there are obvious uncoordinated deformation and stress concentration in the surrounding rock at the interface of soft and hard rock, and the plastic zone of surrounding rock is mainly distributed in the interface of soft and hard rock and soft rock stratum; Zhangziguang [5] et al. Studied the stability of surrounding rock in upper soft and lower hard strata by combining field monitoring and numerical simulation, and put forward the concept of "difficult region (RD1) - easy region (RE) - difficult region (RD2)" according to the difficulty of surrounding rock deformation; Wu Bo [6-9] et al. Studied the failure characteristics of surrounding rock and the quantitative evaluation criteria of surrounding rock stability of tunnels in upper soft and lower hard strata by means of numerical simulation, determined the dual indicators of surrounding rock stability, and established the quantitative evaluation system of surrounding rock stability. D. Stepi[10] et al. Analyzed the progressive failure law of tunnel surrounding rock by means of indoor test and numerical simulation; Ren song [11-12] and others used the nonlinear contact analysis method in ANSYS to analyze the stability of surrounding rock considering the bedding effect; Lichangcheng [13] studied the deformation law of surrounding rock in soft and hard composite strata by summarizing the monitoring data of surrounding rock deformation and surface settlement during Qingdao metro construction; Hexiangfan [14] and others studied the mechanical characteristics of the upper soft and lower hard strata from hard to soft and from soft to hard based on the example of Shenzhen Metro project, and controlled the tunneling parameters accordingly according to the research results; Zhang Dingli [15-16] and others studied the progressive failure characteristics, instability mechanism and instability range of surrounding rock of tunnel in upper soft and lower hard stratum by using the method of model similarity test, numerical simulation and field monitoring data; Li Jing[17] studied the failure mechanism and characteristics of surrounding rock under different dip angles of soft and hard strata and different types of surrounding rock; Chen Hongjun [18] et al. Took Chongqing highway tunnel as the research background, carried out the model test on the failure process of surrounding rock about the inclination degree in the soft and hard composite stratum; Pangweijun[19] and others studied the deformation characteristics of surrounding rock based on the strike dip angle of rock stratum and tunnel, and concluded that there are certain differences in the deformation laws of surrounding rock under different dip angles; Liuhouxiang[20] et al. Studied the influence of lower rock mass on the stability of tunnel surrounding rock under different dip angles by means of finite element numerical simulation; Liuhongbing[21] used the finite difference software FLAC3D to analyze the influence of rock inclination on the stability of tunnel surrounding rock; Shaoyuanyang [22] studied the influence of rock stratum inclination on the stability and failure mode of tunnel surrounding rock by means of numerical simulation; Wang Xiao [23] studied the influence of the dip angle of the fault fracture zone on the stress and deformation of the

tunnel structure by means of numerical simulation, and evaluated the safety of the tunnel structure based on the above research results; Based on different lateral pressure coefficients, Yang Qinghao[24] analyzed the influence of the change of bedding plane inclination on the internal force of the tunnel structure. The results show that the vertical and horizontal in-situ stresses are closer. The more significant the influence of inclination angle on the internal force of tunnel structure; Wang Min[25] studied the influence law of joint dip angle on tunnel surrounding rock deformation under complex geological conditions through the combination of numerical simulation, theoretical analysis and field monitoring; Lai Tiantian[26] and others analyzed the excavation damage deformation of the tunnel bedding hard rock combination surrounding rock under different rock dip angles by means of numerical simulation, and studied the deformation and yield progressive characteristics of the tunnel surrounding rock under different dip angles; Chengaokui[27] analyzed the numerical simulation results under the conditions of different rock dip, and summarized the influence law of rock dip on the stability of surrounding rock of layered rock mass; Li Shuo[28] and others used finite element simulation software to analyze the stress and deformation characteristics of surrounding rock under the conditions of different dip angles of rock strata, and summarized the variation laws of surrounding rock stress and displacement under the conditions of different dip angles of rock strata structural planes; Selby a r[29] studied the ground deformation caused by shield tunnel construction by using linear finite element method and Lagrange finite difference method.

To sum up, scholars at home and abroad mainly study the stability of surrounding rock in composite formation by combining similar model test, numerical simulation and field monitoring data. Most of their research contents are the failure mechanism, failure characteristics and development of plastic zone of surrounding rock stability in composite formation. The impact of dip angle of soft and hard rock interface on the stability of tunnel surrounding rock has not been analyzed, Therefore, in this paper, relying on the actual project of Shenzhen Metro Line 13 Liu~Bai area tunnel crossing the upper soft and lower hard strata, the dip angles of the soft and hard rock interface are set at 0 °, 15 °, 30 °, 45 °, 60 °, 75 ° and 90 ° respectively, and multiple three-dimensional models are established through Midas GTS NX finite element software for calculation and analysis, Thus, the variation law of the surrounding rock deformation and the peak ground settlement when the shield tunnel crosses the upper soft and lower hard stratum under different inclination conditions is obtained. The research results can provide a useful reference for the later practical engineering projects similar to the shield tunnel crossing the upper soft and lower hard stratum. Among them, the technical route is shown in **Figure 1**.

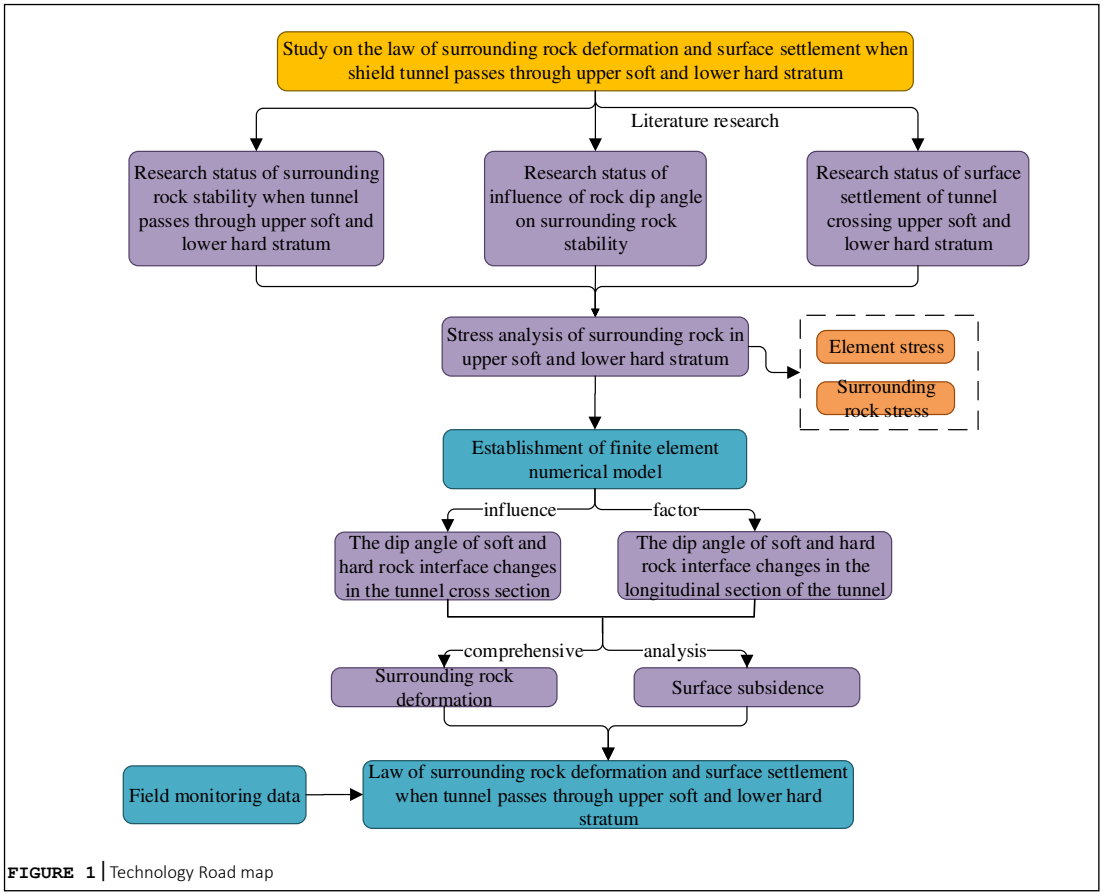

FIGURE 1 | Technology Road map

2 project overview

The stratum structure between Liu~Bai area of Shenzhen Metro Line 13 is complex, there are many kinds of rock and soil mass, and the buried depth, thickness and properties of rock and soil layer change greatly. The tunnel through the stratum mainly includes fill layer, hard plastic soil, fully weathered granite, strongly weathered granite, medium weathered granite, slightly weathered granite, as shown in **Figure 2**. In this paper, the surrounding rocks in the study area are of Class III ~ V, and the Class III surrounding rocks are mainly distributed in ZDK10 + 544 ~ Zdk10 + 561. The Rock Mass at the top of the arch and the surrounding areas are mainly micro-weathered granite, and the surrounding rocks are basically stable. Grade V surrounding rock is mainly distributed in zdk10 + 565 ~ zdk10 + 589 section, the arch crown and surrounding areas are strongly and completely weathered granite, the arch bottom is slightly weathered granite, and the arch crown is prone to local damage without support.

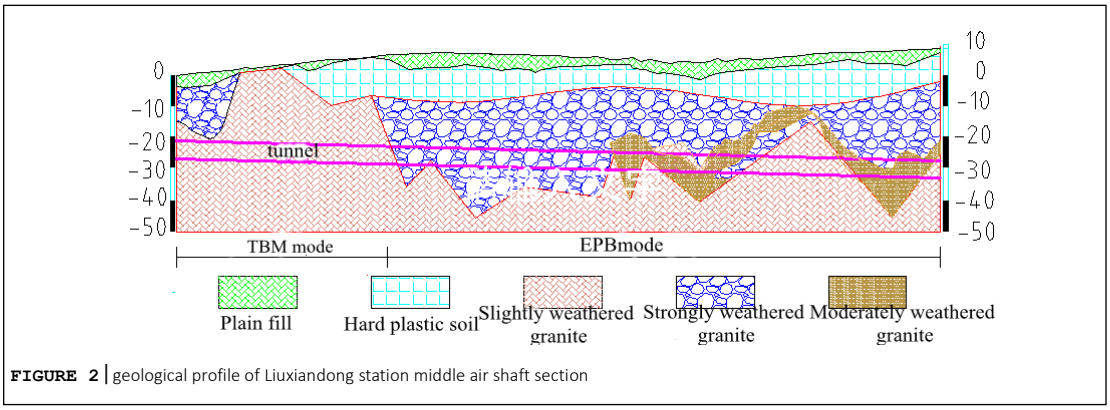

FIGURE 2 | geological profile of Liuxiandong station middle air shaft section

3 Study on variation law of surrounding rock stress when tunnel 2 passes through upper soft and lower hard stratum

According to the research of domestic scholars [33], in the self weight stress field of rock mass, when the buried depth of the tunnel exceeds three times the tunnel diameter, it can be considered that the vertical stress in the upper and lower rock mass of the tunnel is equal. For the convenience of calculation, the overall stress of surrounding rock is decomposed into case 1 and case 2 according to formula (1), so as to ensure that the surrounding rock stress is in an isotropic isobaric state, as shown in **Figure 3**.

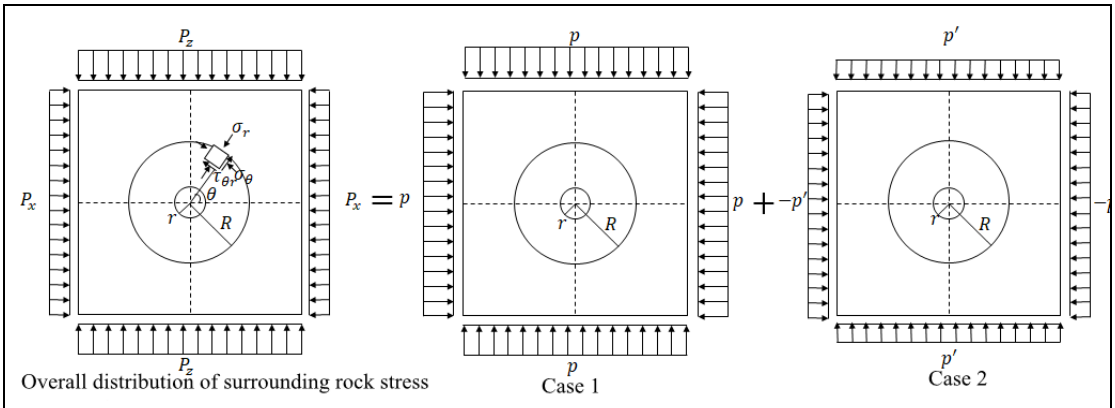

FIGURE 3 | Schematic diagram of load decomposition of tunnel surrounding rock

Type: r is the diameter of the tunnel; R is the radius of the outer circle.

$$\begin{cases} P_z = p + p' \\ P_x = p - p' \end{cases} \quad (1)$$

Solution formula (1) is available:

$$\begin{cases} p = \frac{1}{2}(1+\lambda)P_z \\ p' = \frac{1}{2}(1-\lambda)P_z \end{cases} \quad (2)$$

In the formula, λ is the natural stress ratio coefficient of rock mass.

According to the elastic theory of axisymmetric circular tunnel, when it is symmetrical around the z-axis, the shear stress = 0, it can be introduced that both the tangential and radial stresses of the surrounding rock are the main stress.The tangential and radial stresses of the surrounding rock are shown in formula (3).

$$\begin{cases} \sigma_\theta = P_z\left(1+\frac{r^2}{R^2}\right) \\ \sigma_r = P_z\left(1-\frac{r^2}{R^2}\right) \end{cases} \quad (3)$$

(1) Round rock stress solution in case 1

Since the load of case 1 is axisymmetric, the tangential and radial stress representations of case 1 that are available according to equation (10) ~ (11) are shown as follows:

$$\begin{cases} \sigma_r = p\left(1-\frac{r^2}{R^2}\right) = \frac{1}{2}(1+\lambda)P_z\left(1-\frac{r^2}{R^2}\right) \\ \sigma_\theta = p\left(1+\frac{r^2}{R^2}\right) = \frac{1}{2}(1+\lambda)P_z\left(1+\frac{r^2}{R^2}\right) \end{cases} \quad (4)$$

According to the characteristics that the surrounding rock stress is the main stress and $\sigma_\theta > \sigma_r$, , σ_θ and σ_r can be equivalent to the maximum principal stress and minimum principal stress of surrounding rock , because the tunnel palm surface rock mass is divided into two types of hard rock and soft rock, rock mass cohesion c, internal friction Angle is different, the surrounding rock can bear, the value will change, namely the surrounding rock can withstand main stress σ_1 and σ_3 value changes, especially the soft rock intersection position, surrounding rock main stress value has large fluctuations, easily cause the surrounding strata first damage.

Stress solution of surrounding rock in case 2

When R=r, $\sigma_r = \tau_{\theta r} = 0$;

When $R \to \infty$, the expressions of σ_r and

$\tau_{\theta r}$ can be obtained:

$$\begin{cases}\sigma_r = -p'\cos 2\theta \\ \tau_{\theta r} = p'\sin 2\theta\end{cases} \tag{5}$$

Based on the above boundary conditions and the research results of CAI Meifeng [34] and others, the surrounding rock stress solution of case 2 can be obtained, and its expression is as follows:

$$\begin{cases}\sigma_r = -p'\left(1-4\frac{r^2}{R^2}+3\frac{r^4}{R^4}\right)\cos 2\theta \\ \sigma_\theta = p'\left(1+3\frac{r^4}{R^4}\right)\cos 2\theta \\ \tau_{\theta r} = p'\left(1+2\frac{r^2}{R^2}-3\frac{r^4}{R^4}\right)\sin 2\theta\end{cases} \tag{6}$$

By integrating the surrounding rock stress of case 1 and case 2, the total surrounding rock stress solution can be obtained, and its expression is as follows:

$$\begin{cases}\sigma_r = \frac{1}{2}(1+\lambda)P_z\left(1-\frac{r^2}{R^2}\right)-\frac{1}{2}(1-\lambda)P_z\left(1-4\frac{r^2}{R^2}+3\frac{r^4}{R^4}\right)\cos 2\theta \\ \sigma_\theta = \frac{1}{2}(1+\lambda)P_z\left(1+\frac{r^2}{R^2}\right)+\frac{1}{2}(1-\lambda)P_z\left(1+3\frac{r^4}{R^4}\right)\cos 2\theta \\ \tau_{\theta r} = \frac{1}{2}(1-\lambda)P_z\left(1+2\frac{r^2}{R^2}-3\frac{r^4}{R^4}\right)\sin 2\theta\end{cases} \tag{7}$$

According to the research of Zhang Nianxue [35] and others, the relationship between rock mass cohesion, internal friction angle and Poisson's ratio can be obtained:

$$\begin{cases} c = \frac{\mu\sigma_c}{2(1-\mu)} \\ \mu = \frac{\tan\left(\frac{\pi}{2}-\frac{\varphi}{2}\right)}{1+\tan\left(\frac{\pi}{2}-\frac{\varphi}{2}\right)}\end{cases} \tag{8}$$

Where, σ_c is the uniaxial compressive strength of rock mass.

According to the definition of natural pressure coefficient λ and formula (8), the relationship betweenλ and rock mass cohesion c and internal friction angle φ can be obtained respectively:

$$\lambda_c = 2c/\sigma_c \tag{9}$$

$$\lambda_\varphi = \tan\left(\frac{\pi}{2}-\frac{\varphi}{2}\right) \tag{10}$$

Substituting equation (9) into equation (7) can obtain the relationship between σ_r ,σ_θ and $\tau_{\theta r}$ and rock mass cohesion c:

Substituting equation (9) into equation (7) can obtain the relationship with rock mass cohesion c:

$$\begin{cases}\sigma_r = \frac{1}{2}(1+2c/\sigma_c)P_z\left(1-\frac{r^2}{R^2}\right)-\frac{1}{2}(1-2c/\sigma_c)P_z\left(1-4\frac{r^2}{R^2}+3\frac{r^4}{R^4}\right)\cos 2\theta \\ \sigma_\theta = \frac{1}{2}(1+2c/\sigma_c)P_z\left(1+\frac{r^2}{R^2}\right)+\frac{1}{2}(1-2c/\sigma_c)P_z\left(1+3\frac{r^4}{R^4}\right)\cos 2\theta \\ \tau_{\theta r} = \frac{1}{2}(1-2c/\sigma_c)P_z\left(1+2\frac{r^2}{R^2}-3\frac{r^4}{R^4}\right)\sin 2\theta\end{cases} \tag{11}$$

Substituting equation (10) into equation (7) can obtain the relationship between σ_r , σ_θ and $\tau_{\theta r}$ and internal friction angle ϕ:

$$\begin{cases}\sigma_r = \frac{1}{2}\left[1+\tan\left(\frac{\pi}{2}-\frac{\varphi}{2}\right)\right]P_z\left(1-\frac{r^2}{R^2}\right)-\frac{1}{2}\left[1-\tan\left(\frac{\pi}{2}-\frac{\varphi}{2}\right)\right]P_z\left(1-4\frac{r^2}{R^2}+3\frac{r^4}{R^4}\right)\cos 2\theta \\ \sigma_\theta = \frac{1}{2}\left[1+\tan\left(\frac{\pi}{2}-\frac{\varphi}{2}\right)\right]P_z\left(1+\frac{r^2}{R^2}\right)+\frac{1}{2}\left[1-\tan\left(\frac{\pi}{2}-\frac{\varphi}{2}\right)\right]P_z\left(1+3\frac{r^4}{R^4}\right)\cos 2\theta \\ \tau_{\theta r} = \frac{1}{2}\left(1-\tan\left(\frac{\pi}{2}-\frac{\varphi}{2}\right)\right)P_z\left(1+2\frac{r^2}{R^2}-3\frac{r^4}{R^4}\right)\sin 2\theta\end{cases} \tag{12}$$

It can be seen from the above formula that when the tunneling stratum changes from homogeneous hard rock to homogeneous soft rock, the cohesion and internal friction angle of rock mass gradually decrease, and the radial stress value and tangential stress value show a gradually decreasing trend, this shows that the pressure release rate of surrounding rock in soft rock stratum is large after tunnel excavation, especially the settlement deformation of arch crown is greatly affected by the

value of σ_r. The higher the stress release rate, the greater the settlement deformation caused by tunnel excavation. Therefore, it is not difficult to infer that the stress distribution of surrounding rock in upper soft and lower hard stratum is quite different from that in homogeneous stratum. Specifically, the stress release degree of tunnel surrounding rock in soft rock is significantly higher than that in hard rock, which causes the stress value of the former to be less than that of the latter at the same position, resulting in the disharmony of surrounding rock stress distribution, Thus, the plastic zone and deformation zone of surrounding rock after tunnel excavation are mainly distributed in the surrounding rock with poor properties.

The cross-sectional strata of the tunnel are distributed as shown in **Figure 4**. The soft-hard rock interface rotates anticlockwise around the plumb line in **Figure 4**. The angle between the solid red line and the horizontal line in Figure 4 is α and varies from $0^\circ \sim 90^\circ$.

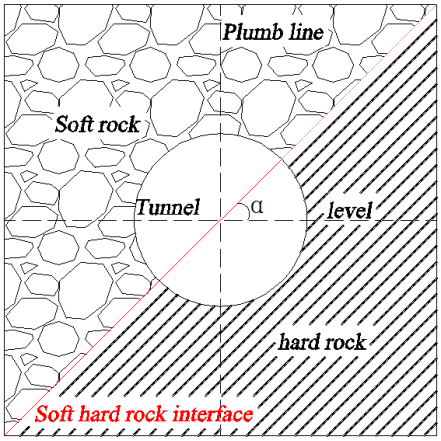

FIGURE 4 | Schematic diagram of the soft and hard rock junction surface in the cross section of the tunnel

It can be seen from **Figure 4** that with the continuous increase of the included angle α, the rock mass located on the left side of the plumb line gradually becomes soft rock, resulting in a gradual increase in the proportion of soft rock in the tunnel rock mass on the left side of the plumb line. According to formula (11) ~ (12), the surrounding rock stress that the tunnel on the left side of the plumb line can bear is very easy to reach its own extreme stress value. The surrounding rock was the first to fail. After the left side rock is damaged, a new active load will be formed on the right side rock of the tunnel, which will induce the damage of the right side rock of the tunnel.

4 Numerical simulation of shield tunnel passing through upper soft and lower hard stratum

4.1 Establishment of numerical model of shield tunnel passing through upper soft and lower hard stratum

The types of rock and soil mass encountered during tunnel construction are complex. The interface between soft and hard rock cannot be guaranteed to be in a horizontal state all the time, resulting in randomness in the type and distribution of rock and soil mass on the face. However, the current numerical simulation method cannot completely restore the type and proportion of the rock and soil mass on the face during the tunnel excavation process. Reasonable simplification and assumption of site geological conditions and construction methods. The specific simplification and assumptions are as follows: (1) it is assumed that the rock and soil mass is a continuously distributed isotropic material, and the concrete material is assumed to be a continuous linear elastic material, ignoring its nonlinear characteristics; (2) The three-dimensional numerical model only

considers the self weight stress of rock and soil mass, and does not consider the influence of soil structural stress on tunnel construction; (3) It is assumed that when the dip angle of the soft and hard rock interface changes in the tunnel cross section, the soft and hard rock interface passes through the center of the tunnel circle, and the tunnel is divided into two parts with equal volume; (4) It is assumed that when the inclination of the interface between soft and hard rock changes in the longitudinal section of the tunnel, the midpoint of the tunnel axis coincides with the midpoint of the interface between soft and hard rock, so as to ensure that the stratum crossed by the tunnel during construction is the upper soft and lower hard composite stratum. The grid division diagram of shield tunnel crossing the upper soft and lower hard stratum is shown in **Figure 5**.

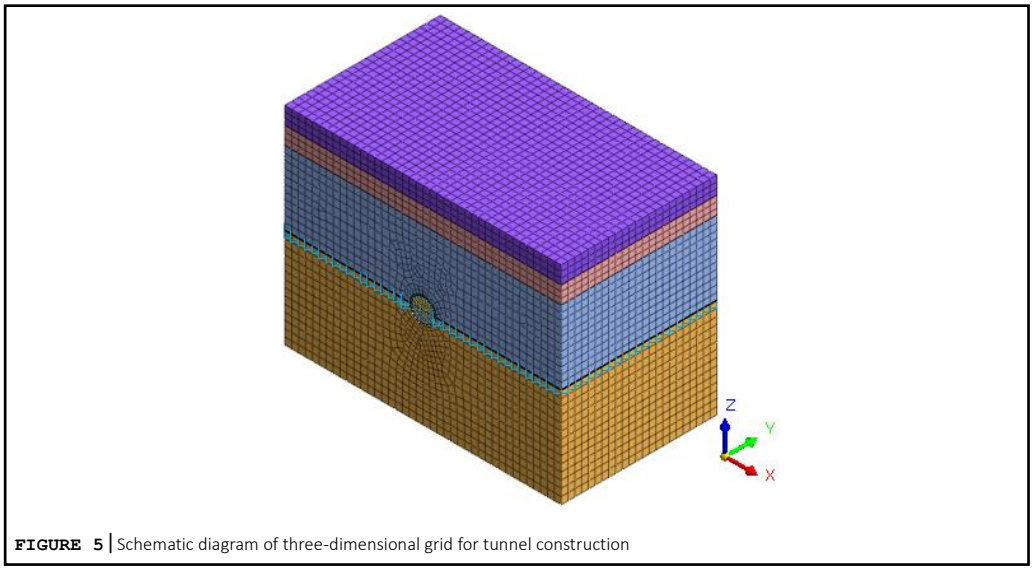

FIGURE 5 | Schematic diagram of three-dimensional grid for tunnel construction

4.2 Selection of physical and mechanical parameters such as rock, soil and lining structure

In this paper, the effect of groundwater seepage during tunnel construction is studied in small areas, so the influence of groundwater on tunnel construction is not considered. The tunnel surrounding rock mainly includes slightly weathered mixed granite and strongly weathered mixed granite. The overlying rock and soil mainly includes hard plastic soil, plain fill and strongly weathered granite. The physical and mechanical parameters of rock and soil, equivalent layer and lining structure are shown in **Table 1**, The calculation parameters of interface elements are shown in Table 2. According to the research of Xu Yingjin [36], the calculation formula of concrete equivalent layer is shown in formula (13). In this paper, according to the actual shield project of liuxiandong station ~ Baimang station of Shenzhen Metro Line 13, the thickness of equivalent layer is taken as 300mm.

$$\delta = (1+\mu)\Delta \qquad (13)$$

Where, Δ is the clearance value of shield tail, δ is the thickness of equivalent layer, and μ is the conversion coefficient, which is generally in the range of 0.7 ~ 3.0.

Table 1 | Table of physical and mechanical parameters of rock and soil body and lining structure

Formation type	γ (kN · m-3)	E(Mpa)	φ(°)	c(Kpa)	u
Plain fill	18	40	8	12	0.15
Hard plastic soil	18	41	20	28	0.29

Microweathered granite	27	40000	/	/	0.20
Strong weathering granite	20	1000	27	50	0.27
duct piece	26	34500	/	/	0.20
Equgeneration (before elastic-slurry hardening)	20	1200	/	/	0.20
Equgeneration (after elastic-slurry hardening)	23.7	3000	/	/	0.20

Table 1| Interface unit

Interface unit	The tangential stiffness/(kN/m3)	Normal stiffness/(kN/m3)	φ(°)	c(Kpa)
Soft and hard rock handover surface	3×108	2.8×108	15	27

4.3 Simulation condition setting

The tunnel in this section is excavated by shield method. In order to better restore the interface of upper soft and lower hard composite stratum encountered in the process of tunnel construction, the inclination change of soft and hard rock interface is divided into two situations: the change of tunnel cross section and the change of tunnel longitudinal section. On this basis, the inclination of soft and hard rock interface is set to seven working conditions: 0 º, 15 º, 30 º, 45 º, 60 º, 75 º and 90 º respectively, The influence of the dip angle of the interface between soft and hard rock on the deformation of tunnel surrounding rock and surface settlement is studied. The specific construction steps are as follows:

Case 1: analysis of surrounding rock deformation and surface settlement when the inclination of soft and hard rock interface changes in the direction of tunnel cross section.

Working condition I (the dip angle of soft and hard rock interface is 0 º):

(1) According to the interface of soft and hard rock in the direction of tunnel cross section, the tunnel crossing stratum is divided into two types: slightly weathered mixed granite and strongly weathered mixed granite;

(2) Initial stress field simulation. Activate the rock and soil grid element, self weight stress and boundary constraints, simulate the initial stress of the stratum, and clear the initial displacement;

(3) In order to more effectively analyze the impact of changes in geological conditions on tunnel construction, the tunnel is excavated in 15 stages. In each stage, the number of shield propulsion rings is 2. Passivate the soil unit and equivalent layer unit of the first 2 rings of the tunnel, activate the corresponding lining unit, and add grouting pressure at the segment; Then passivate the grouting pressure and change the properties of equivalent layer to simulate the slurry hardening process;

(4) Passivate the tunnel face pressure applied in the previous step, and repeat step (3) until the tunnel excavation is completed.

Condition 2 ~ condition 7:

Set the dip angles of soft and hard rock interface to 15 º, 30 º, 45 º, 60 º, 75 º and 90 º respectively, and repeat the operation of condition 1 until the tunnel excavation is completed.

The working condition setting of case 2 is the same as that of case 1.

5 Analysis of numerical simulation results of shield tunnel passing through upper soft and lower hard strata

5.1 Analysis of influence of dip angle of soft and hard rock interface on vertical stress of surrounding rock

To study the influence of the inclination of soft and hard rock cross angle in the tunnel cross section, section I-I is located in the positive direction along the X axis, the section of Y axis 21m is named section II-II, as shown in **Figure 6**.

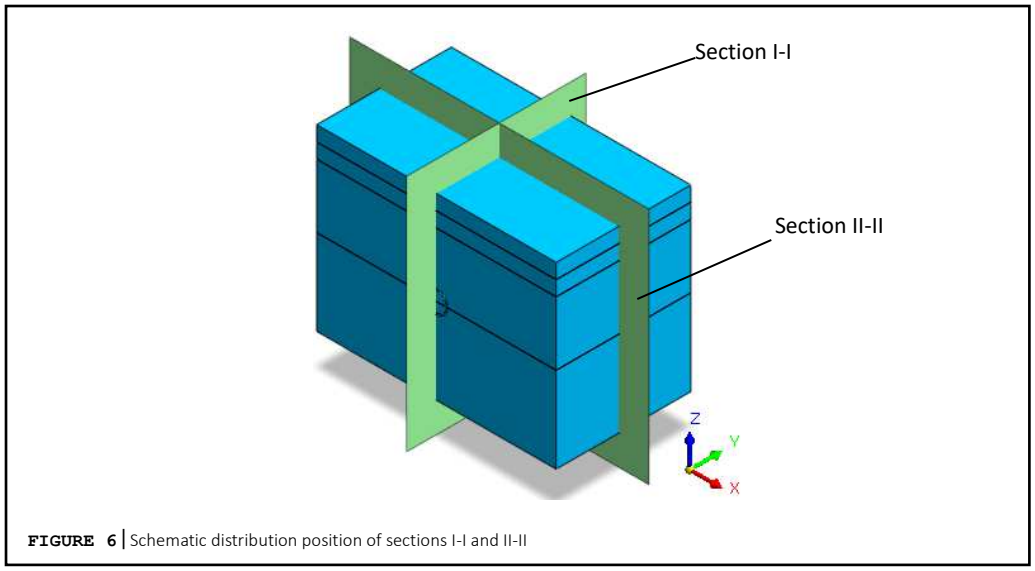

FIGURE 6 | Schematic distribution position of sections I-I and II-II

To analyze the change of vertical stress of surrounding rock, the index of "Mises stress" is introduced to study the change of vertical stress of surrounding rock caused by tunnel excavation under different dip angles. As the vertical stress of surrounding rock changes slowly under different dip angles, the vertical stress of surrounding rock with dip angles of 0 º, 30 º, 60 º and 90 º is selected for analysis, as shown in **Figure 7**.

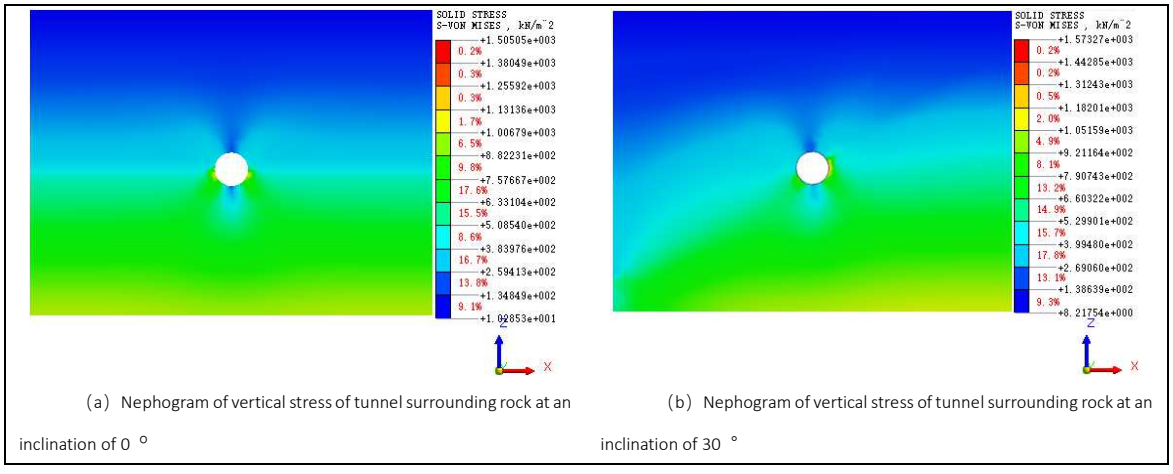

(a) Nephogram of vertical stress of tunnel surrounding rock at an inclination of 0 °

(b) Nephogram of vertical stress of tunnel surrounding rock at an inclination of 30 °

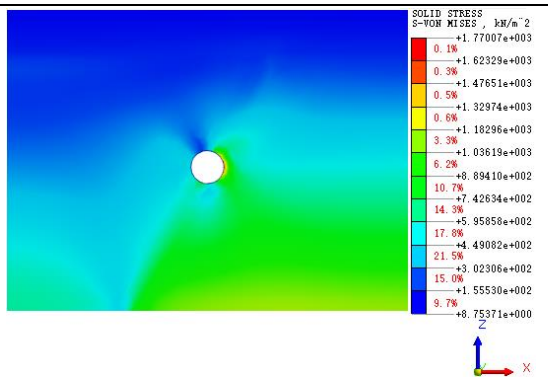

(c) Nephogram of vertical stress of tunnel surrounding rock at an inclination of 60 °

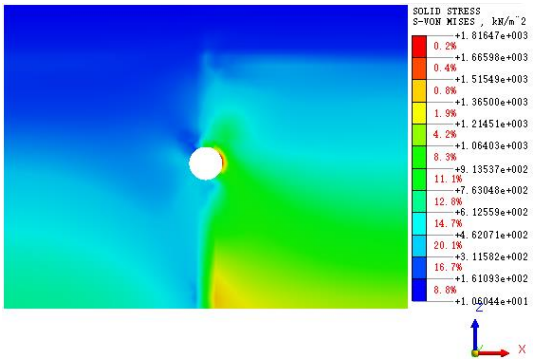

(d) Nephogram of vertical stress of tunnel surrounding rock at an inclination of 90 °

FIGURE 7 | cloud chart of vertical stress of tunnel surrounding rock under different dip angles

It can be seen from the vertical stress nephogram of the tunnel surrounding rock under different dip angles: (1) When the dip angle is 0°, the formation stress is approximately distributed in layers, and the intersection of the soft and hard rocks on the left and right sides of section I-I faces the formation stress. The division effect is basically the same. When the dip angle is greater than 0°, compared with the soft and hard rock interface on the right side of section I-I, the interface between soft and hard rocks on the left side of section I-I has a more significant division effect on formation stress; (2) When the dip angle is 0° When the inclination angle is greater than 0°, the stress concentration degree of the surrounding rock on the right side of the section I-I is obviously higher than that of the surrounding rock on the left side; (3) With the continuous increase of the inclination, the stress concentration area of the surrounding rock on the left side of the tunnel shows a downward trend, and the stress concentration area of the surrounding rock on the right side of the tunnel shows an upward trend. The number of stress concentration areas of the surrounding rock of the tunnel gradually changes from two to one, and gradually approaches the right arch waist of the tunnel. According to the analysis, the above phenomenon is directly related to the change of the dip angle of the interface between soft and hard rocks.

It can be seen from the above analysis results that the dip angle of the soft and hard rock interface has a great impact on the distribution characteristics of the vertical stress concentration area of the surrounding rock, but the impact of the dip angle change on the vertical stress value is not analyzed. Therefore, the vertical stress values of the vault, arch bottom, left arch waist and right arch waist at tunnel section ii-ii are selected to analyze the impact of the dip angle on the above characteristic points, as shown in **Figure 8**.

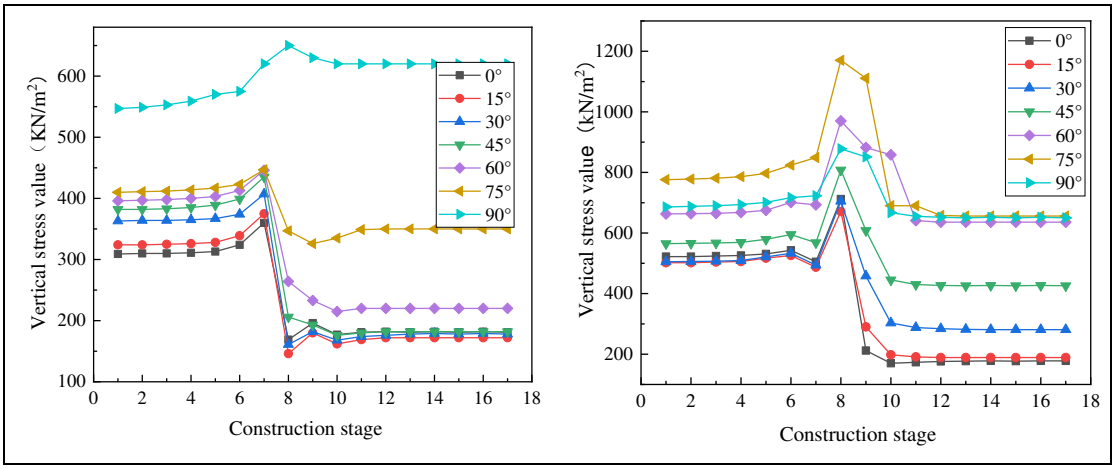

(a) Vertical stress curve of arch under different inclination conditions

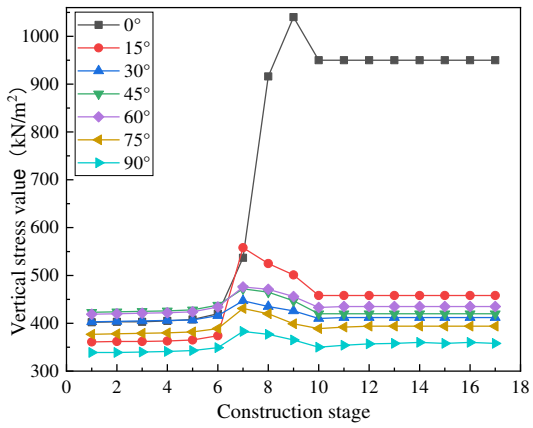

(b) Vertical stress curve diagram of the arch bottom under different inclination conditions

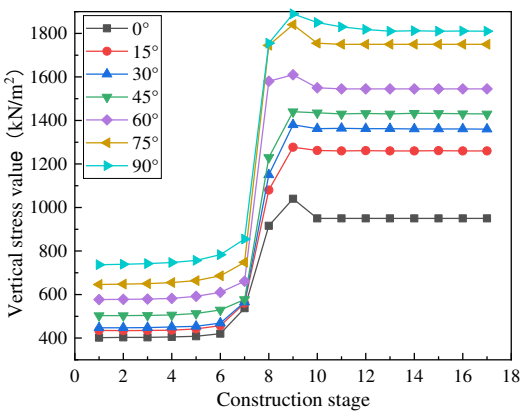

(c) Vertical stress graph of the left arch waist under different inclination conditions

(d) Vertical stress curve diagram of the right arch waist under different inclination conditions

FIGURE 8 | Plot of vertical stress change under different inclination conditions of soft and hard rock junction surface

As can be seen from **Figure 8a** , firstly, the initial and final values of the vertical stress of the vault increase with the increase of the dip angle, the maximum variation range is from 75°to 90°. Secondly, the vertical stress release rate of vault decreases gradually from 40% to 14.6% when the dip angle varies from 0°to 75°.When the dip angle is 90°, the final value of the vertical stress of the vault is greater than the initial stress value. The analysis shows that with the continuous increase of the dip angle, the distance between the vault and the hard rock stratum gradually shortens, resulting in the gradual reduction of the stress state release rate. When the inclination angle is 90°, the strata on the left and right sides of the tunnel are soft rock and hard rock respectively. After the tunnel is excavated, the vertical stress concentration area is mainly distributed in the hard rock stratum, so the phenomenon of stress concentration occurs when the inclination angle is 90° .It can be seen from **Figure 8b** that, firstly, the vertical stress release at the arch bottom is caused by construction stage 9, while the stress release at the arch crown is mainly caused by construction stage 8. There is a certain difference between the two stages of stress release. The analysis shows that section ii-ii is located at the junction of construction stage 8 and construction stage 9. After the completion of construction stage 8, the settlement deformation trend of the arch crown rock mass is higher than the uplift deformation trend of the arch bottom [15-16], The stress release of the arch crown is one stage ahead of that of the arch bottom; Secondly, the vertical stress release rate of the arch bottom in the range of 0 ° ~45 ° is significantly higher than that in the range of 60 ° ~90 °, and the stress release rate reaches the lowest when the inclination is 90 °, which is about 9.8%; Finally, after the completion of tunnel excavation, the dip angles corresponding to the maximum and minimum vertical stress at the arch bottom are 75 ° and 0 ° respectively, and the difference between the two is 520kN/m^2. It can be seen that the change of dip angle of soft and hard rock interface has a great impact on the vertical stress at the arch bottom.

It can be seen from **Figure 8c** to **Figure 8d**. First of all, after the tunnel construction is completed, the vertical stress value of the right arch waist is generally greater than that of the left arch waist, and it increases with the inclination angle. The vertical stress difference between the left and right arch waist shows a gradually expanding trend[33]-[34]. The analysis shows that the greater the inclination angle is, the more significant the difference in the properties of the left and right arch

waist strata is, The surrounding rock stress transferred to the right arch waist is higher than that transferred to the left arch waist, which leads to the occurrence of the above phenomenon; Secondly, after the completion of tunnel excavation, the stress state at the left and right arch waist is stress concentration, which is quite different from the stress state at the arch crown and arch bottom. The analysis shows that after the tunnel excavation is completed, the vault and the vault are unloaded, and the surrounding rock stress gradually spreads to the left and right sides, resulting in a gradual increase in the stress at the left and right arch waists. Finally, there is a large difference in the vertical stress values between the 0° inclination angle at the left arch waist and other inclination angles.The analysis shows that with the continuous increase of the inclination angle, the proportion of soft rock at the left arch waist gradually increases, and the maximum bearing capacity of soft rock is less than that of hard rock, which leads to the above phenomenon.

5.2 Analysis of the influence of the dip angle of the soft and hard rock interface on the equivalent plastic strain of the surrounding rock in the tunnel cross section

In order to study the influence of tunnel excavation on the plastic deformation of surrounding rock under different dip angles of soft and hard rock interface, the index of "equivalent plastic strain" is introduced to analyze the distribution law of equivalent plastic strain of surrounding rock under different dip angles, and the plastic yield position of surrounding rock of tunnel is obtained. The cloud diagram of medium effect plastic strain is shown in **Figure 9**.

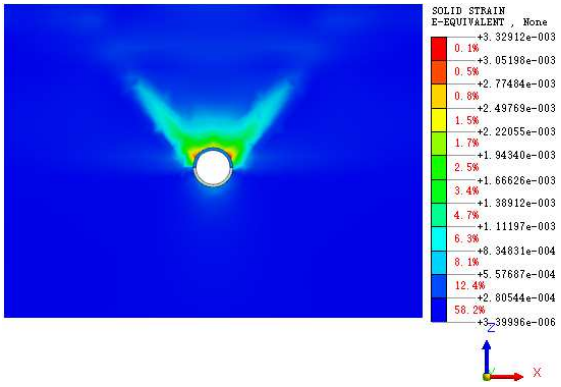

(a) Cloud diagram of the equivalent plastic strain of the tunnel surrounding rock when the inclination angle is 0

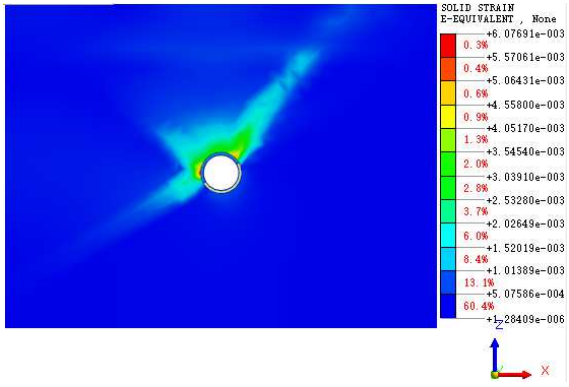

(b) Cloud diagram of the equivalent plastic strain of the tunnel surrounding rock when the inclination angle is 30

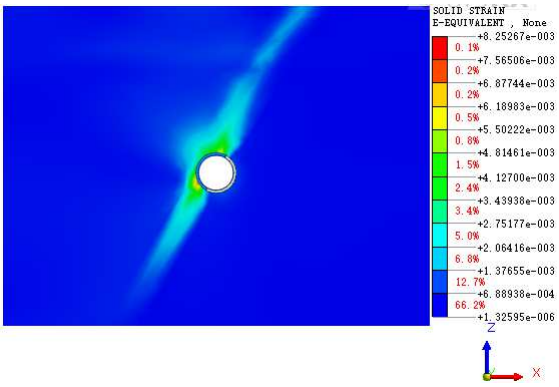

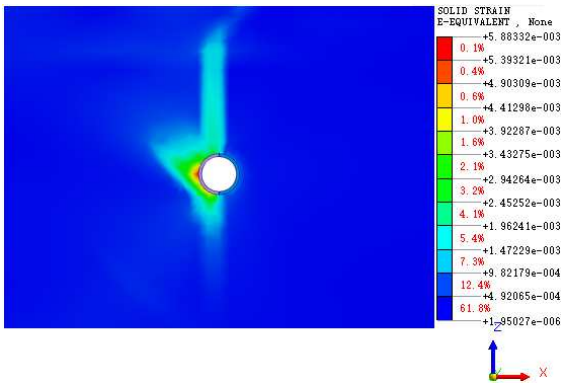

(c) Cloud map of the equivalent plastic strain of the tunnel surrounding rock at an inclination angle of 60

(d) Cloud map of the equivalent plastic strain of the tunnel surrounding rock when the inclination angle is 90

FIGURE 9 | Cloud map of tunnel surrounding rock under different inclination conditions

It can be seen from the equivalent plastic strain nephogram of tunnel surrounding rock under different dip angles. Firstly, the equivalent plastic strain concentration area caused by tunnel construction is mainly distributed at the interface between soft rock stratum and soft and hard rock. The overall distribution characteristics of the strain concentration area on the left side of section I-I are wide and short, and the overall distribution characteristics on the right side are narrow and long [6-9], The dip angle of soft and hard rock interface has a significant influence on the distribution characteristics of equivalent plastic strain concentration area of surrounding rock [4]; Secondly, with the continuous increase of the dip angle of the soft and hard rock interface, the equivalent plastic strain gradually penetrates to the surface along the soft and hard rock interface in the process of upward transmission. With the continuous increase of the dip angle of the soft-hard rock interface, the equivalent plastic strain gradually penetrates to the surface along the soft-hard rock interface in the process of upward transmission, and its transmission distance increases first in the process of downward transmission. trend of decreasing afterward. The transmission distance reaches its maximum value when the inclination angle is 60°. Finally, the dip angle of the soft and hard rock interface has a certain influence on the number and distribution of the equivalent plastic strain red area. Specifically, when the dip angle is within the range of 0 ° ~ 30 °, there are two distribution positions of the red area of equivalent plastic strain, both of which are distributed from the arch waist to the arch crown. When the dip angle is within the range of 30 ° ~ 60 °, the distribution position of the red area of equivalent plastic strain is gradually reduced from two to one, It is mainly distributed from the left arch waist to the arch bottom. When the inclination angle is within the range of 60 ° ~ 90 °, there is only one red area of equivalent plastic strain, and its distribution position gradually moves from below the left arch waist to near the left arch waist. To sum up, the distribution position of the maximum value of equivalent plastic strain on the left side of the tunnel shows a trend of moving down first and then up, and the peak value and distance of equivalent plastic strain reach the maximum at the inclination angle of 60 °.

5.3 Analysis of influence of dip angle of soft and hard rock interface on surrounding rock deformation

When analyzing the influence of the inclination angle of the soft and hard rock interface on the vertical deformation of the surrounding rock of the tunnel, since the change trend between adjacent inclination angles is relatively slow, the vertical deformation cloud map of the surrounding rock of 0^o , 30^o , 60^o , and 90^o is selected for analysis, as shown in **Figure 10**.

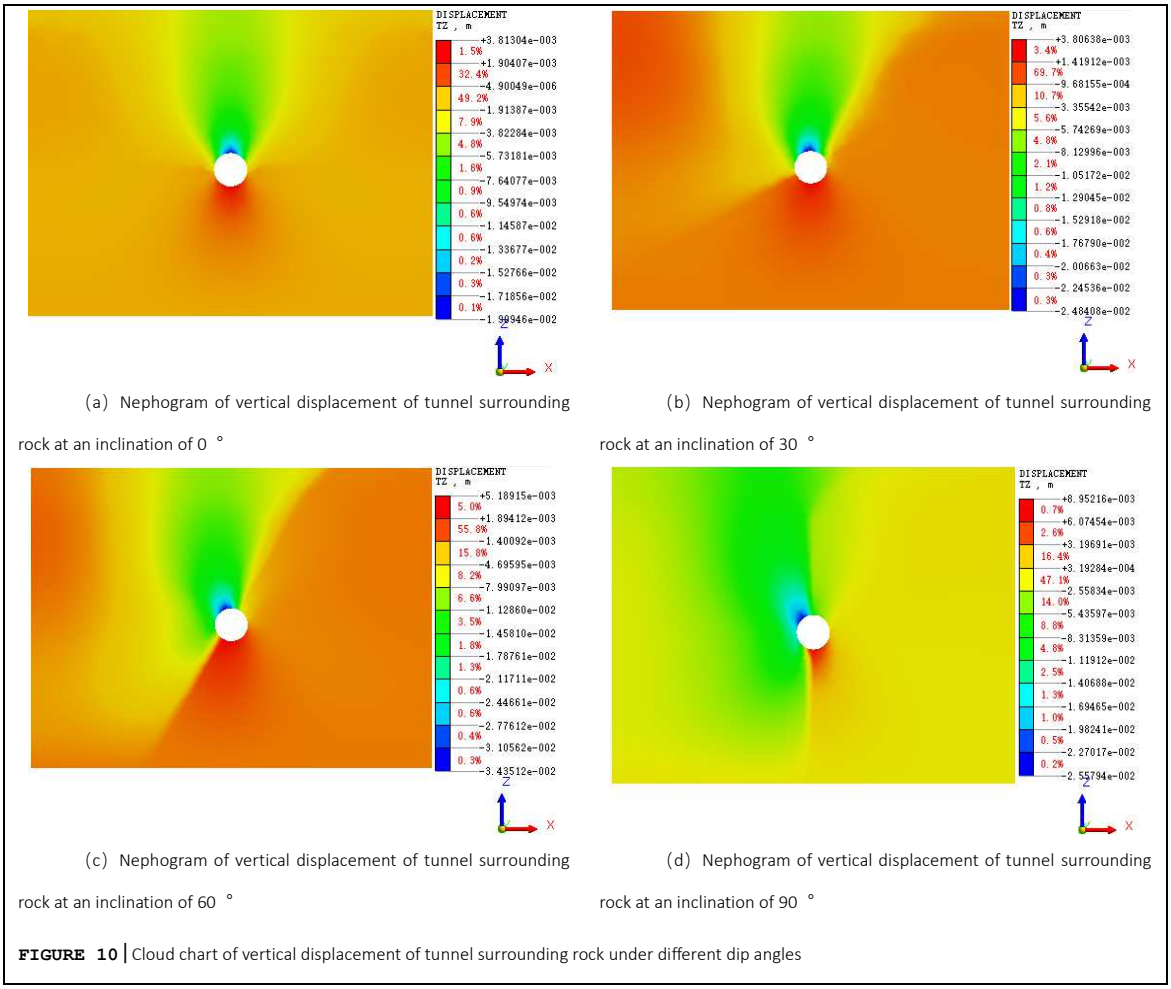

(a) Nephogram of vertical displacement of tunnel surrounding rock at an inclination of 0 °

(b) Nephogram of vertical displacement of tunnel surrounding rock at an inclination of 30 °

(c) Nephogram of vertical displacement of tunnel surrounding rock at an inclination of 60 °

(d) Nephogram of vertical displacement of tunnel surrounding rock at an inclination of 90 °

FIGURE 10 | Cloud chart of vertical displacement of tunnel surrounding rock under different dip angles

According to the vertical displacement nephogram of tunnel surrounding rock under different dip angles, (1) with the continuous increase of the dip angle of the soft and hard rock interface, the settlement deformation concentration area at the tunnel crown shows a counterclockwise movement trend, which is close to the rotation trend of the soft and hard rock interface. The specific performance is as follows: when the dip angle is within the range of 0 ° ~30 °, the movement trend is relatively slow, and when the dip angle is within the range of 60 ° ~90 °, the movement trend is significantly accelerated; (2) With the continuous increase of the inclination angle, the area of the deformation area at the vault of the tunnel shows a gradual increase trend, and the relationship between the areas of the deformation area of the vault on the left and right sides of section I-I gradually changes from approximately equal to that on the left side is larger than that on the right side, while the area of the deformation area at the bottom of the arch shows a trend of first increasing and then decreasing, and the relationship between the areas of the deformation area of the vault on the left and right sides of section I-I is just opposite to that of the vault; (3) With the continuous increase of the dip angle of the soft and hard rock interface, the rotation angle of the surrounding rock deformation concentration area on the left side of section I-I is basically the same as that of the soft and hard rock interface, and there is a certain difference in the rotation angle of the surrounding rock deformation area on the right side. The specific performance is that when the dip angle is within the range of 0 ° ~30 °, the rotation angle is smaller than that of the soft and hard rock interface, and when the dip angle is within the range of 60 ° ~90 °, The rotation angle is basically the same as that of the interface.

In order to deeply study the influence of the dip angle of the soft and hard rock interface on the vertical deformation of the tunnel surrounding rock,

the vertical deformation values of four characteristic points at the vault, arch bottom, left arch waist and right arch waist of the tunnel section ii-ii are selected for analysis, as shown in **Figure 11**.

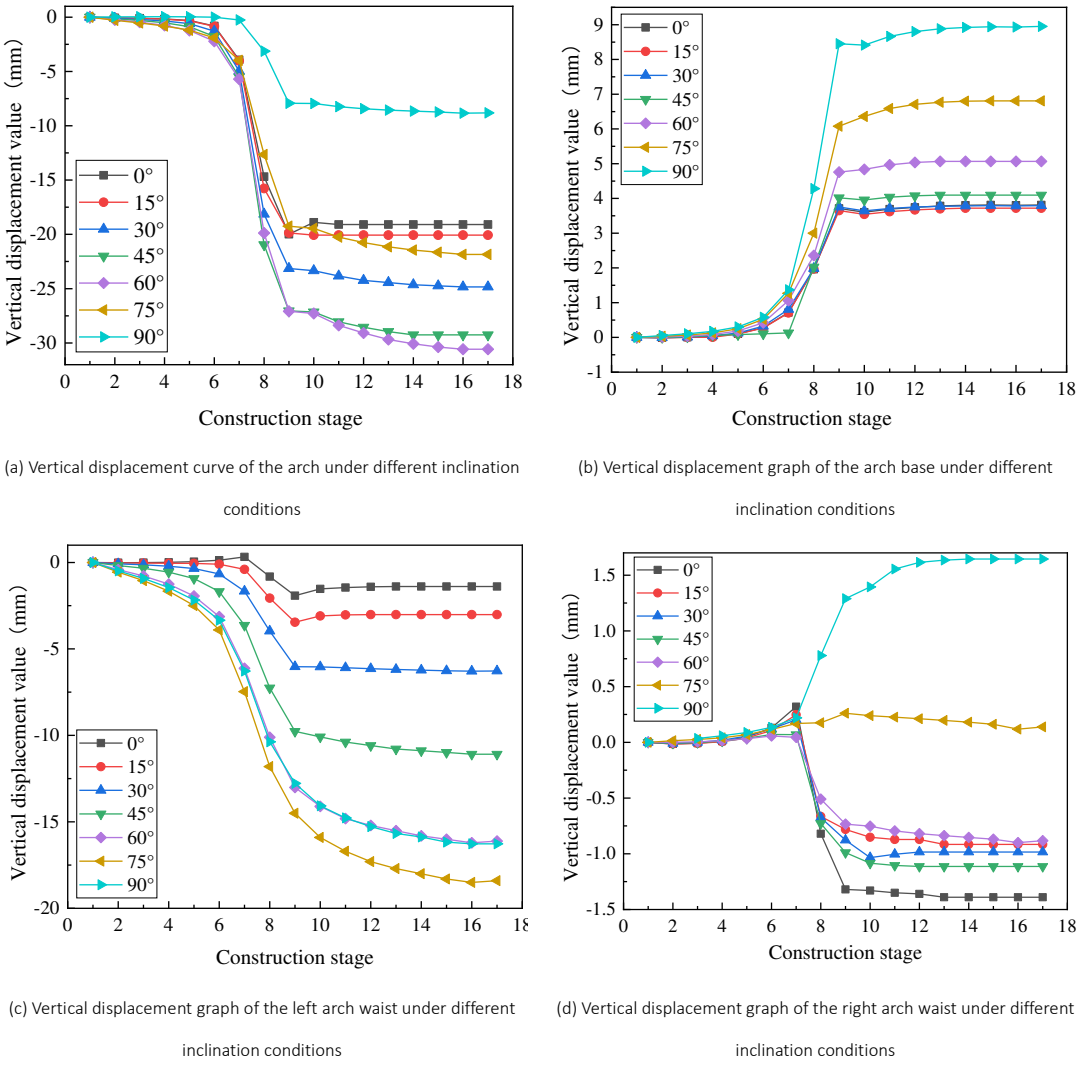

(a) Vertical displacement curve of the arch under different inclination conditions

(b) Vertical displacement graph of the arch base under different inclination conditions

(c) Vertical displacement graph of the left arch waist under different inclination conditions

(d) Vertical displacement graph of the right arch waist under different inclination conditions

FIGURE 11 | Vertical displacement curve of surrounding rock under different inclination conditions

It can be seen from **Figure 11a** that, first, with the increasing inclination, the vertical displacement of the arch crown shows a trend of increasing first and then decreasing, reaching the maximum value at the 60 ° inclination. According to the analysis of Fig. 10, it can be seen that the main reason for the above-mentioned change trend of the vertical displacement of the vault is that the distribution position of the vertical displacement concentration area at the vault changes with the change of the inclination angle. Secondly, the peak vertical displacements of the vault under different inclination angles are 19.09mm, 20.07mm, 24.84mm, 29.25mm, 30.58mm, 21.85mm and 8.81mm, respectively. From the above data, it can be seen that the peak value of the vertical displacement changes the most in the range of 15 ° ~30 ° dip angle, with a change range of about 23.8%, and the smallest in the range of 75 ° ~90 ° dip angle, with a change range of about -59.7%.

As can be seen from **Figure 11b**, first, when the dip angle of the interface between soft and hard rock is within the range of 0 ° ~30 °, the vertical displacement curve of the arch bottom basically coincides, and the peak value of the vertical displacement is stable at about 3.75mm. The analysis shows that when the dip angle is within the

range of 0 ° ~30 °, hard rock accounts for more in the rock mass on the left and right sides of the arch bottom. Compared with soft rock, its anti disturbance ability is stronger, resulting in a relatively small change range of the vertical displacement of the arch bottom within the dip angle range; Secondly, when the dip angle of the soft and hard rock interface is within the range of 45 ° ~90 °, the vertical displacement value of the arch bottom shows a positive correlation with the dip angle, and the deformation difference of the arch bottom uplift between adjacent dip angles is also positively correlated with the variation law between dip angles, especially in the range of 60 ° ~90 °, the deformation difference of the arch bottom uplift between adjacent dip angles increases significantly, This shows that the inclination angle, which has a great influence on the vertical displacement of the arch bottom, is mainly distributed in the range of 60 ° ~90 °; Thirdly, according to the analysis of **Figure 11a**, with the continuous increase of the inclination of the interface between soft and hard rocks, there is a certain difference in the change trend of the vertical displacement curve of the arch crown and the arch bottom. The analysis shows that the above phenomenon is closely related to the distribution position of the vertical displacement concentration area in Fig. 11.

From **Figure 11** (c) to **Figure 11** (d), it can be seen that, first, with the continuous increase of the inclination angle, the vertical displacement value of the left arch waist shows a trend of first increasing and then decreasing, and reaches the maximum value at 75 °; Secondly, with the continuous increase of inclination angle, the vertical displacement value at the right arch waist gradually changes from negative value to positive value, which shows that the vertical deformation at the right arch waist gradually changes from settlement deformation to uplift deformation. The analysis shows that with the continuous increase of inclination angle, the concentration area of uplift deformation caused by tunnel excavation gradually changes from the uniform distribution on the left and right sides of section I-I to the area mainly distributed on the right side of section i-i, The settlement deformation concentration area gradually changes from the uniform distribution on the left and right sides of section I-I to the main distribution on the left side of the arch crown, resulting in the uplift deformation effect on the right arch waist is greater than the settlement deformation effect, resulting in the positive vertical deformation of the right arch waist when the inclination is 90 °; Thirdly, when the inclination angle is 75 °, the vertical displacement value of the right arch waist is basically 0, and the vertical displacement value of the left arch waist reaches the maximum value, which shows that the 75 ° inclination angle is the safest inclination angle of the right arch waist and the most dangerous inclination angle of the left arch waist.

5.4 Verification and analysis of numerical simulation results and engineering monitoring data.

In this paper, zdk10+544.32~zdk10+589.32 mileage between Liubai district and Baiqu District of Shenzhen Metro Line 13 is taken as the monitoring interval, and zdk10+565.32 is selected as the monitoring section. The stratum conditions of the monitoring section are plain fill, hard plastic soil, strongly weathered mixed granite and slightly weathered mixed granite from top to bottom. The buried depth of the tunnel crown is 28m, the surrounding rock grade is III ~ IV, and the dip angle of the soft and hard rock interface of the monitoring section is 60 °.

From the numerical simulation results in Section 4.3, extract the simulation value of tunnel crown settlement when excavating to section ii-ii, collect the monitoring data of crown settlement when the left line tunnel is excavated to section zdk10+565.32, and compare and analyze the above two groups of data, as shown in **Figure 12**.

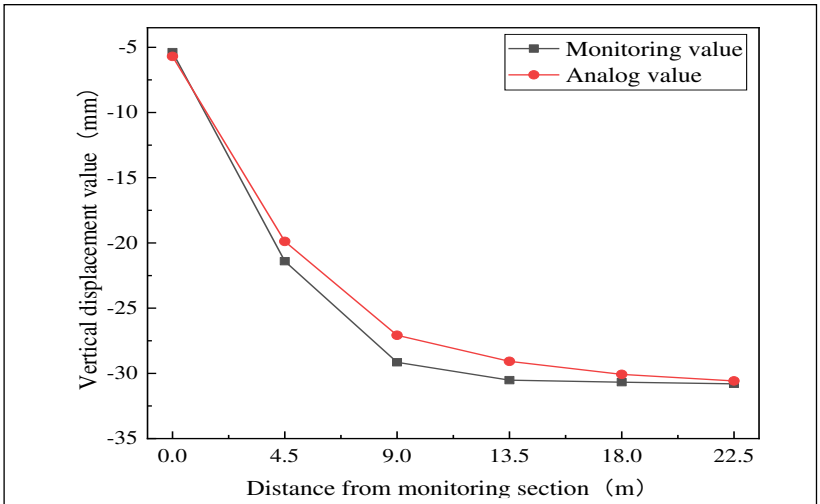

FIGURE 12 | Curve of arch crown settlement simulation value and monitoring value

It can be seen from **Figure 12** that, first of all, the curve change trend of the simulated value and the monitored value is roughly the same, but the monitored value of the vault settlement is slightly larger than the simulated value. The analysis shows that the constitutive model of rock and soil mass and the selected parameter values in the finite element numerical simulation are different from the rock mass in the actual project, and the tunnel construction steps are simplified in the process of numerical simulation. The above reasons lead to the numerical simulation value being smaller than the field monitoring value, But in general, the error between the two is less than 20%, which verifies the accuracy of the numerical simulation results to a certain extent.

6 Conclusion

The finite element simulation software Midas GTS NX is used to simulate the construction process of the tunnel passing through the upper soft and lower hard strata, and the influence of the inclination angle of the soft and hard rock interface on the deformation of the surrounding rock is studied when the tunnel passes through the upper soft and lower hard strata. The accuracy of the numerical simulation results is verified by the field monitoring data. The specific conclusions are as follows:

(1) The influence of the dip angle of the soft and hard rock interface in the tunnel cross section on the surrounding rock stress, the equivalent plastic strain of surrounding rock and the surrounding rock deformation is studied, and the variation law of the surrounding rock stress and the surrounding rock deformation value is analyzed. The research results show that: 1) with the continuous increase of the dip angle, the surrounding rock stress, the equivalent plastic strain of surrounding rock and the distribution law of the surrounding rock deformation concentration area change, There are significant differences between the left and right sides of the interface between soft and hard rocks; 2) There are great differences in the variation trends of surrounding rock stress and displacement at the arch crown, arch bottom, left and right arch waist under different inclination conditions, but the peak value of horizontal displacement and vertical displacement both show a variation trend of increasing first and then decreasing, and reach the maximum value when the inclination is 60 °, in which the horizontal displacement is mainly concentrated near the left arch waist, and the vertical displacement is mainly concentrated near the arch crown and arch bottom.

(2) The vault settlement simulation value is compared with the monitoring value, and the following conclusions are drawn: 1) the variation trend of the vault settlement monitoring value curve is basically the same as that of the vault settlement simulation value curve. The vault settlement monitoring value is slightly larger than the vault

settlement simulation value, and the error of the two is not more than 20%. To a certain extent, it also verifies the rationality and feasibility of the numerical simulation.

From the above analysis, it can be concluded that the variation of dip angle of soft and hard rock interface in the cross section of tunnel has a significant effect on the deformation of surrounding rock and the surface settlement, it can be concluded that the study of the dip angle of soft and hard rock joint can provide certain reference for the construction of similar projects in the later stage. However, this paper mainly studies the influence of the dip angle of the soft and hard rock interface on the single track tunnel. In the later research, we can continue to study the influence of the dip angle of the soft and hard rock interface on the surrounding rock deformation and surface settlement in the case of double track tunnel.

Reference

[1] Chen Wei, Hong Kairong, Jiao Shengjun, et al Shield construction technology [m] Beijing: People's Communications Press, 2016

[2] Lei x y Swoboda. Application of Contact-Friction Interface Element to Tunnel Application of contact-friction Excavation in Faulted Rock[J]. Computers and Geotechnics, 1995, 17(3): 349-370. doi: 10.1016/0266-352X(95)99217-F

[3] Yassaghi A,Salari-rad H. Squeezing Rock Conditions at an Igneous Contact Zone in the Taloun Tunnels Tehran-shomal Freeway[J]. International Journal of Rock Mechanics and Mining Sciences, 2005, 42(1): 95-108. doi:10.1016/j.ijrmms. 2004.07.002

[4] Wang Wei, Deng Huafeng, pan Deng, et al Influence of the distribution of soft and hard rock layers on the stability of tunnel surrounding rock [j] Highway transportation technology, 2019, 36 (7): 106-113, 120 doi:CNKI:SUN:GLJK. 0.2019-07-013

[5] Zhang Ziguang, Qiu Wenge Study on three-dimensional regional division of urban underground space stability in Qingdao [j] Journal of underground space and engineering, 2018, 14 (4): 881-892 doi:CNKI:SUN:BASE. 0.2018-04-003

[6] Wu Bo, Wang Mingtao, Deng Zheng Study on stability factors and influence of tunnels in upper soft and lower hard strata [j] Journal of underground space and engineering, 2019, 15 (2): 589-600 doi:CNKI:SUN:BASE. 0.2019-02-036

[7] Wu Bo, Huang Wei, Wu Bingbing Research Progress on stability mechanism and quantitative evaluation of tunnels in composite strata [j] Science, technology and engineering, 2020, 20 (33): 13529-13537 doi:10.3969/j.issn. 1671-1815.2020.33.003

[8] Wu Bo, Wang Mingtao, Huang Wei Study on quantitative evaluation criteria of tunnel surrounding rock stability in upper soft and lower hard strata [j] Modern tunnel technology, 2019, 56 (1): 114-123 doi:10.13807/j.cnki. mtt. 2019.01.017

[9] Wu Bo, Huang Wei, Wang Wangyang, et al Research on risk assessment of tunnel construction in upper soft and lower hard strata based on PRA method [j] Journal of natural disasters, 2018, 27 (4): 26-33 doi:CNKI:SUN:ZRZH. 0.2018-04-004

[10] D.sterpi,A.cividini. A Physical and numerical investigation on the stability of shallow tunnels in strain softening media[J]. Rock Mechanics and Rock Engineering, 2004, 37(4): 277-298. doi:10.1007/s00603-003-0021-0

[11] Ren song, ouyangxun, Jiang Deyi, et al Stability analysis and initial support optimization of soft and hard interbedded tunnel [j] Journal of Huazhong University of science and Technology (NATURAL SCIENCE EDITION), 2017, 45 (7): 17-22 doi:10.13245/j.hust. one hundred and seventy thousand seven hundred and four

[12] Ren song, Li Yu, ouyangxun, et al Dynamic simulation method and construction method optimization of surrounding rock of horizontal soft and hard interbedded tunnel [j] Journal of Xi'an University of architecture and Technology (NATURAL SCIENCE EDITION), 2018, 50 (3): 317-323 doi:CNKI:SUN:XAJZ. 0.2018-03-002

[13] Li Changcheng Study on deformation law of surrounding rock in soft and hard cluster formation [j] Building technology development, 2017, 44 (7): 160-161 doi:CNKI:SUN:JZKF. 0.2017-07-104

[14] He Xiangfan, Shen Xingzhu, Wang Fan, et al Analysis of mechanical characteristics of shield tunnel construction through upper soft and lower hard strata [j] Railway standard design, 2017, 61 (2): 89-95 doi:10.13238/j.issn. 1004-2954.2017.02.020

[15] Zhang Dingli Analysis of tunnel surrounding rock stability and its supporting effect [j] Journal of Beijing Jiaotong University, 2016, 40 (4): 9-18 doi:10.11860/j.issn. 1673-0291.2016.04.002. doi:10.11860/j.issn. 1673-0291.2016.04.002

[16] Zhang Dingli, Sun Zhenyu Stability and control of

surrounding rock structure of complex tunnel [j] Journal of hydropower, 2018, 37 (2): 1-11 doi:10.3969/j.issn. 1672-5093.2018.05.058

[17] Li Jing Study on failure mechanism and evaluation of surrounding rock of tunnel in upper soft and lower hard stratum [d] Fuzhou University, 2017

[18] Chen Hongjun, Liu Xinrong, Wang Cheng, et al Study on surrounding rock stress in the failure process of inclined soft and hard interbedded tunnel [j] Modern tunnel technology, 2017, 54 (4): 68-76 doi:10.13807/j.cnki. mtt. 2017.04.009

[19] Pang Weijun, Xia Zhongkang, Jiao Haiping Influence of the strike angle between rock stratum and tunnel on the deformation characteristics of surrounding rock [j] Journal of railway engineering, 2019, 36 (7): 52-57 doi:CNKI:SUN:TDGC. 0.2019-07-010

[20] Liu Houxiang, Zheng Zhixiong, Hu Yongjun, et al Analysis of the influence of different dip angles of layered rock mass on the stability of high ground stress tunnel [j] Transportation Science and engineering, 2014, 30 (2): 46-50 doi:10.3969/j.issn. 1674-599X. 2014.02.008

[21] liuhongbing Analysis of the influence of rock dip on the stability of layered rock tunnel [j] Highway engineering, 2013, 38 (4): 167-169, 182 doi:CNKI:SUN:ZNGL. 0.2013-04-040

[22] shaoyuanyang Study on surrounding rock stability and failure mode of layered rock tunnel [d] Southwest Jiaotong University, 2013 doi: 10.7666/d.Y2319867

[23] Wang Xiao Stability analysis and construction parameter optimization of tunnel in fault fracture zone [d] Beijing Jiaotong University, 2017 doi:CNKI:CDMD:2.1017.278868

[24] Yang Qinghao Study on stress characteristics of tunnel structure considering creep effect of layered surrounding rock [d] Southwest Jiaotong University, 2018 doi:CNKI:CDMD:2.1018.977100

[25] Wang min Deformation characteristics of near horizontal sedimentary surrounding rock of tunnel dominated by steep dip joints [d] Xiangtan University, 2013 doi:10.7666/d.D351729

[26] Lai Tiantian, Lei Hao, Liu Zhiqiang, et al Study on surrounding rock excavation deformation of deep buried hard rock tunnel with different rock inclination [j] Journal of railway engineering, 2020, 37 (7): 69-76

[27] Chen gaokui Comprehensive study on surrounding rock stability of layered rock tunnel [d] Fuzhou University, 2014

[28] Li Shuo, Wang Haibo, Zhao Xiaoxue, et al Numerical simulation study on deformation characteristics of layered rock tunnel [j] Journal of Anhui University of science and Technology (NATURAL SCIENCE EDITION), 2019, 39 (6): 65-72 doi:CNKI:SUN:HLGB. 0.2019-06-013

[29] Selby A R. Tunnelling in soils–ground movements, and damage to buildings in Workington, UK[J]. Geotechnical and Geological Engineering, 1999, 17(3): 351-371. doi:10.1023/A:1008985814841

[30] Ling Xianchang, caidesuo Rock mechanics [m] Harbin: Harbin Institute of Technology Press, 2002

[31] Cai Meifeng, he ManChao, Liu Dongyan Rock mechanics and engineering [m] Beijing: Science Press, 2002

[32] Zhang nianxue, Sheng Zhuping, Li Xiao, et al Research on the relationship between rock Poisson's ratio and internal friction angle [c]/ / Proceedings of the 11th (2011) academic annual meeting of Institute of Geology and Geophysics, Chinese Academy of Sciences (middle), 2012: 112-122 doi:CNKI:SUN:YSLX. 0.2011-S1-001

[33] Xu Yingjin Study on tunnel and ground settlement caused by shield construction under synchronous grouting and its control [d] Beijing Jiaotong University, 2019

[34] Wang Zhijie, Li Zhen, Xu Haiyan, et al Study on the influence of dip angle on the stability of surrounding rock in soil sand interbedded strata [j] Journal of railway engineering, 2019, 36 (9): 54-59, 84 doi:CNKI:SUN:TDGC. 0.2019-09-010

[35] Wang Rui, Zhao Zhiqing, Deng Xianghui, et al The scope and distribution of the loose zone of tunnel excavation in layered surrounding rocks with different dip angles [j] Railway construction, 2019, 59 (9): 65-67 doi:CNKI:SUN:TDJZ. 0.2019-09-016